Pharmaceutical Research (© 2006)
DOI: 10.1007/s11095-006-9749-z

Research Paper

Near-Infrared Spectrometry for the Quantification of Dermal Absorption of Econazole Nitrate and 4-Cyanophenol

Joseph Medendorp,[1] Jhansi Yedluri,[1] Dana C. Hammell,[1] Tao Ji,[1] Robert A. Lodder,[1] and Audra L. Stinchcomb[1,2]

Received November 3, 2005; accepted December 13, 2005

Purpose. The purpose of this study was to demonstrate the utility of near-infrared (NIR) spectroscopy for the *in vitro* quantification of econazole nitrate (EN) and 4-cyanophenol (4-CP) in hairless guinea pig skin.
Methods. NIR spectra were collected from each of the following: EN and 4-CP powders, EN and 4-CP in solution, and skin samples following topical exposure to either 4-CP in water or EN in propylene glycol and topical creams. To predict drug concentration from NIR spectra, principal component regression (PCR), interval PCR, and uninformative variable elimination PCR were each used with a leave-one-out cross-validation, and results were compared. NIR results were validated against known skin concentrations measured by high-pressure liquid chromatography (HPLC) analysis of solvent extracts.
Results. NIR results matched the HPLC results for the quantification of 4-CP and EN in skin exposed to saturated solutions and topical creams with an $r^2 > 0.90$, a standard error of estimation <7.0%, and a standard error of performance < 8.0%.
Conclusion. This experiment demonstrated that NIR closely parallels results obtained from tissue extraction and HPLC analysis, proving its potential utility for the rapid and noninvasive determination of topical bioavailability/bioequivalence of EN and quantification of the model chemical 4-CP. Investigation of drugs in human skin is now justified.

KEY WORDS: dermal drug absorption; interval principal component regression (iPCR); PCR–uninformative variable elimination (PCR-UVE); topical bioequivalence.

INTRODUCTION

Application. Methods to determine the bioequivalence of drugs from topical administration have been discussed formally by the FDA for many years (1). A vasoconstrictor assay measuring skin blanching has been used to determine the bioequivalence of topical steroids (2). This steroid blanching is the only topical bioequivalence test that has been agreed upon among the majority of the topical drug delivery scientists. Punch biopsies of the dermis and epidermis have been performed to determine skin drug concentrations in humans *in vivo*, but this is very invasive and leaves permanent scarring. Sampling of just the stratum corneum using tape stripping has generated the most interest of all the current methods under investigation; however, this method has many variables and intricacies that result in inter- and intralab variation (3). One problem noted with tape stripping is that the chemical continues to diffuse through the skin sample in the time it takes to collect the tape strips. In addition, tape stripping is not ideal for volatile chemicals, as they tend to evaporate faster than the required analysis time. As an alternative to processing the tape strips with solvent extraction and high-pressure liquid chromtography (HPLC) analysis, attenuated total reflectance–Fourier transform infrared spectroscopy (ATRFTIR) has been used to quantify chemicals on the tape with some degree of success (4–6). The tape stripping technique is not exactly noninvasive, as substantial skin irritation is also generated by complete removal of the stratum corneum. Microdialysis has also been explored for topical bioequivalence measurement, but this is also a relatively invasive and inflammation-inducing procedure (7). Noninvasive imaging techniques of the skin have become more popular over the last few years (8). Currently, *in vitro* human skin drug-diffusion studies are performed to study topical drug products. In these experiments, tissue samples are often extracted whole or sectioned and extracted, and then the solvent

[1] Department of Pharmaceutical Sciences, College of Pharmacy, University of Kentucky, 725 Rose Street, Lexington, KY 40536-0082, USA.
[2] To whom correspondence should be addressed. (e-mail: astin2@email.uky.edu)

extract is analyzed by HPLC or some other analytical method for drug content. The skin-sample analysis time doubles both the duration of the experiment and its total cost.

There is a significant need to find a noninvasive and simple method to determine topical drug product bioequivalence. There is also a substantial need for a method of topical drug-product development research with an instrument, serving as an easier way to analyze and image skin drug concentrations and cutting development time and cost in half.

The best solution, however, in terms of time and ease of application is an all-optical approach. A rapid all-optical approach effectively eliminates the possibility of continued diffusion while scanning. In addition, different volatilities of chemicals are less relevant because scans are collected instantaneously from all depths in the skin sample. For these reasons, near-infrared (NIR) spectrometry was chosen as the method of analysis.

Photonic techniques can detect and measure chemically and medically significant optical parameters not accessible to other clinical imaging modalities (9,10). However, in contrast to X-rays, for example, the use of optical methods to probe human tissue properties presents major problems because human tissue is decidedly scattering, which sets up uncertainty in the interpretation of transmission and scattering data.

A number of types of experiments have been utilized in medical applications. One is the continuous-wave (CW) experiment employed in this research. In a CW experiment, a continuous modulated beam (often a laser) injects photons into a tissue-like skin, and the intensity of reradiated light on the same surface is measured as a function of distance from the injection point. A second kind of experiment entails time gating, in which, after a pulse of photons is injected in the tissue, the reradiated photons are measured at a fixed distance from the injection point as a function of time. Models for these experiments normally presume that the tissue is semi-infinite and bounded by a planar surface. This is typically a fine assumption because photons at the energies used are able to penetrate only a few millimeters of the tissue. A third kind of experiment, not particularly useful in skin studies *in vivo*, is termed the transillumination experiment. In transillumination, photons traverse a thin slab of tissue. Measurements of the transmitted light are made either with a steady input beam or as a function of time.

Because tissue is greatly scattering, theory must be applied to decipher the measurements. The most rigorous formulation of the theory entails solving a transport equation (TE). Solving the TE involves intense computation, and because scattering cross sections can only be approximated, these calculations are not used as frequently as calculations based on photon diffusion theory or random walk theory (11,12). Unluckily, diffusion theory is intrinsically inaccurate in close proximity to interfaces, which exist in skin. A further impediment to use of optical diffusion theory is that it cannot imitate very short-time ballistic behavior, which can include important information in time-gated experiments, and which would also be required to achieve depth resolution in skin.

Instrumentation. Econazole nitrate (EN) and 4-cyanophenol (4-CP) were chosen as the analytes for the following research. 4-CP is a model chemical with an NIR chromophore unique from skin (4). Both compounds exhibit strong NIR chromophores; thus, it is a simple matter to analyze their spectra. Because NIR can have a tissue penetration depth of many millimeters, it has previously been used in studies for the noninvasive analysis of drugs in tissue (13). It has also been used to quantify the depth of photon penetration in tissues (14,15).

A future instrument already under construction will replace the bulky full spectrum NIR with a small and portable handheld device termed as a solid-state spectral imager (SSSI). It is composed of an aluminum block with three concentric rings of light-emitting diodes (LEDs). Each ring has a different diameter and is centered on a single lead sulfide photodetector. With different angles of incidence, each ring has a different angle of skin penetration. To be collected at the photodetector, light from the ring farthest from the center must penetrate the skin more deeply than from the ring closest to the center. Although only one signal is collected, the LEDs are frequency modulated such that the contribution of each individual LED can be deconvolved from the total signal. In this manner, a spectral profile can be constructed at different depths in the tissue, allowing for the rapid determination of drug penetration.

Theory. A three-dimensional version of the TE for the electric field E can be calculated using Maxwell's equations. Assuming a constant charge density, Maxwell's equations are as follows:

$$\mu\frac{\partial H}{\partial t} = -\nabla \times E, \quad \sigma E + \varepsilon\frac{\partial E}{\partial t} = \nabla \times H \tag{1}$$

where $\boldsymbol{\sigma}$ is the conductivity, $\varepsilon\varepsilon$ is the dielectric permittivity, and μ is a parameter expressed in terms of impedance (12). If H is removed from these equations, then E fulfills the three-dimensional *TE*

$$\frac{\partial^2 E}{\partial t^2} + \frac{\sigma}{\varepsilon}\frac{\partial E}{\partial t} = \frac{1}{\mu\varepsilon}\nabla^2 E \tag{2}$$

NIR models for chemical composition based on scattering data are generally derived statistically based on calibration data, and as such are incomplete without a description of the multivariate statistics needed to

analyze the results. In search for the most descriptive model, the present research explored the use of a number of different chemometric approaches including principal component regression (PCR) (16), interval PCR (iPCR), and PCR–uninformative variable elimination (PCR-UVE) (17,18). For each of these models, principal components were calculated by a singular value decomposition of matrix **A** according to:

$$\mathbf{A} = \mathbf{U}\,\mathbf{S}\,\mathbf{V} \tag{3}$$

where **A** is the matrix of original spectra, **U** is the matrix of eigenvalues (scores), **S** is a diagonal matrix of singular values, and **V** is the matrix of eigenvectors (loadings). As shown in Eq. (4), a regression of **U** indicates which of the components have the strongest correlation to a change in drug concentration **y**, where a is the y-intercept, **b** is a vector of regression coefficients, and c is the residual.

$$\mathbf{y} = a + \mathbf{b}\mathbf{U} + c \tag{4}$$

Equation (5) demonstrates how a leave-one-out cross-validation can be used to predict the concentration of topical drug present from the NIR spectra, where $\boldsymbol{\sigma}^2$ is the variance and $f_i(\mathbf{U}_i)$ is the prediction of the model for the *i-th* pattern m in the training set, after it has been trained on the $m - 1$ other patterns.

$$\boldsymbol{\sigma}^2_{LOO} = \frac{1}{m}\sum_{i=1}^{i=m}(y_i - f_i(\mathbf{U}_i))^2 \tag{5}$$

In the case of a simple two-component system, it is a simple matter to observe a linear change in the analyte concentration. When only two system components are present, only one principal component is needed to describe the concentration change accurately. The loading corresponding to this principal component accurately reflects the contribution of each wavelength to the overall classification. However, in complex systems, such as tissues, where many system components change simultaneously, multiple principal components are needed for the prediction model.

Interval PCR performs the same analysis as above except on smaller subsets of the data set rather than the data set in its entirety (18). For example, when the experimenter specifies an interval (I) of 200 wavelengths, the algorithm performs PCR followed by principal component selection and cross-validation on intervals of 200. By using a moving boxcar, all wavelengths are paired with all other wavelengths inside of ±I. For example, after the algorithm analyzes 1501–1700 nm, the next iteration analyzes 1502–1701 nm, and so on. At the final wavelength, the first I wavelengths are added to the end for the final iterations. In this manner, each wavelength is included in a new model I * 2 times. The goal of interval selection is the minimization of the standard error of performance (SEP) in Eq. (6), which indicates the interval with the highest correlation to the change in drug concentration:

$$SEP = \frac{\left(\frac{c^2}{n-1}\right)^{1/2}}{\max(R) - \min(R)} \tag{6}$$

where c is the residual, n is the number of spectra, and R is a concentration vector.

From the description of iPCR, it is apparent that while one interval may give an acceptable predictive ability, it does not take into account the interaction among variables and peaks outside of the specified interval. PCR-UVE compensates for this by randomly selecting combinations of I variables (18). Loading vectors are retained and summed for each combination of variables so that every variable contains a weight from a number of different local models. The final loading vector indicates the individual wavelengths with the highest correlation to the desired change in drug concentration. The variables with the largest loading are used in the final calibration with the ultimate goal of minimizing the SEP.

MATERIALS AND METHODS

Materials. 4-Cyanophenol, Hanks' balanced salts modified powder, sodium bicarbonate, and propylene glycol were purchased from Sigma (St. Louis, MO, USA). EN, 4-(2-hydroxyethyl)-1-piperazineethanesulfonic acid (HEPES), gentamicin sulfate, trifluoroacetic acid (TFA), triethylamine (TEA), potassium phosphate (monobasic, anhydrous), hydrochloric acid, polyethylene glycol 400 (PEG), methanol, and acetonitrile (ACN) were obtained from Fisher Scientific (Fair Lawn, NJ, USA). 1-Octane sulfonic acid sodium salt was purchased from Chrom Tech® (Apple Valley, MN, USA).

Donor Solutions and Creams. Saturated donor solutions of EN were prepared in propylene glycol (20 mg/ml). Saturated donor solutions of 4-CP were prepared in nanopure water (35 mg/ml). One percent EN creams were used from four different manufacturers: Manufacturer 1, 2, 3, 4 for the 4 creams. Propylene glycol, nanopure water, and a placebo cream were also investigated to collect skin spectra from vehicle interference.

In Vitro Diffusion Studies. Teflon MatTek Permeation Devices (MPD, MatTek Corporation, Ashland, MA, USA) were used for the *in vitro* skin diffusion studies. The MPD is essentially a modified form of a Franz diffusion cell that is meant to be used

for *in vitro* tissue culture permeation studies. It is a practical diffusion cell choice because it requires a smaller amount of valuable skin and it has a portable and unbreakable Teflon design, as opposed to the larger glass Franz cells, which must be used on a large water-circulating/stirring bench. Spacers are used in the wells of the diffusion cells to hold the skin in place. Three MPDs were used for each treatment (donor solution/cream) and exposure time (three per formulation treatment), for a total of nine MPDs per formulation treatment. The purpose of the different exposure times was to create different skin concentrations for measurement and correlation. The receiver solution (simulated "blood flow" compartment under the skin in the MPD) was composed of 60% Hanks' pH 7.4 buffer and 40% PEG. The PEG is added to the buffer to help solubilize hydrophobic drugs without damaging the skin.

The diffusion studies were conducted with dermatomed (split thickness, ~250 μm) hairless guinea pig skin. Skin samples were stored at −20°C until use. Animal use was approved by the University of Kentucky Institutional Animal Care and Use Committee. Hairless guinea pig skin was used for these experiments instead of human skin to develop and validate the methodology in a tissue that is more readily available and economical than human tissue. Hairless guinea pigs are the best small animal model skin match to human skin for diffusion studies (19). Skin samples were secured into the MPD and placed in a tightly sealed glass chamber with 10 ml of the receiver solution so that the level of receiver solution remained constant and in contact with the dermis side of the skin. Donor solutions of 200 or 400 μl of cream were added directly onto the stratum corneum from the upper opening of the cell. To prevent the evaporation of the donor solution, cells were capped with vial caps (Waters, Milford, MA, USA). Microstirring bars were centered below each diffusion cell and set to stir at a constant rate throughout the experiment. At the end of the diffusion experiment, skin samples were removed from the diffusion cells and rinsed with nanopure water three times for 10 s each. In the case of the creams, an alcohol wipe was used to remove excess surface formulation gently. Samples were placed on a paper towel and blotted, then two tape strips (Scotch™ Book Tape 845) were performed to remove surface drug. The skin was rinsed once more with nanopure water, blotted dry with paper towel, and the treated skin area was excised from the center of the skin sample. NIR analysis followed immediately.

Skin Extraction and HPLC Analysis. Immediately following NIR analysis, the tissue was weighed. The sample was then minced with a scalpel and placed in a vial with 5 ml of ACN. This vial was then sonicated for 10 min and shaken for 15 h at 32°C to extract the drug from the tissue into the ACN. The tissue extract was then analyzed for drug concentration by HPLC analysis and expressed as micrograms of drug per wet gram of tissue weight.

HPLC assay was performed with a Perkin-Elmer Series 200 Autosampler, Pump, Column Oven, and a 785A ultraviolet/visible (UV/VIS) Detector with Turbochrom Professional Version 4.1 Software. A Brownlee® C18 RP Spheri–5-μm column (220 × 4.6 mm) with a C18 RP 7-μm guard column (15 × 3.2 mm) was used with the UV/VIS Detector set at a wavelength of 215 nm for EN and 246 nm for 4-CP. The mobile phase used for EN was 70:30 ACN/25 mM potassium phosphate buffer with 0.65 g/l 1-octane sulfonic acid sodium salt. The mobile phase used for 4-CP was 50:50 ACN/0.1% TFA adjusted with TEA to a pH of 3.0. The flow rate of the mobile phase was at 1.5 ml/min for EN and 1.0 ml/min for 4-CP with 100- and 30-μl injections of the sample, respectively. Standards were analyzed with each set of diffusion samples and exhibited excellent linearity over the concentration range employed. The retention times for EN and 4-CP were 5.94 ± 0.05 and 3.33 ± 0.04 min, respectively. The sensitivity of each assay was 25 ng/ml.

NIR ANALYSIS

Drug Powders. Pure powders were scanned first to ensure that EN and 4-CP had distinct NIR chromophores. A uniform layer of pure drug approximately 1 mm thick was loaded on a one-well depression microscope slide (Gold Seal Products, Portsmouth, NH, USA). NIR spectra from 1100 to 2500 nm were collected in steps of 2 nm (1100, 1102, 1104,...) with an NIR spectrometer (Technicon InfraAlyzer 500, Tarrytown, NY, USA) interfaced to a computer (OptiPlex GXM 5166, Dell, Round Rock, TX, USA) running SESAME 3.1 (Bran + Luebbe, Norderstedt, Germany). Scans were collected inside the instrument drawer. To maximize light scatter, microscope slides and samples were placed on top of a conical reflecting cup, designed such that when a sample is placed along the axis of radial symmetry of the cone, specular reflection at the detector is minimized, whereas diffuse reflectance is maximized (20). All data were exported to Matlab 7.0.1 (The Mathworks Company, Natick, MA, USA) for processing and analysis. Samples were each scanned three times, rotating them 120° between each scan.

Drugs in Solution. To demonstrate how effectively NIR could predict drug concentrations from NIR spectra of drugs in solution, spectra were collected from EN and 4-CP in 75% ACN and 25% buffer/PEG receiver solution. The drug that diffuses through the skin can be analyzed in the receiver solution diluted

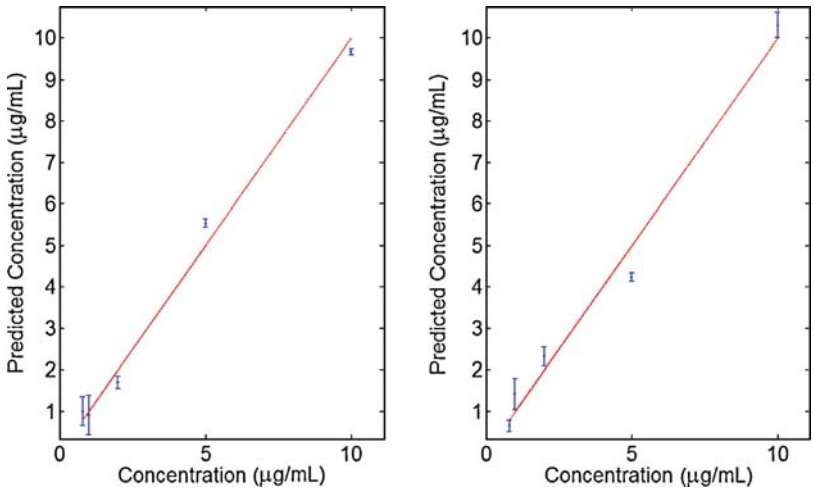

Fig. 1. Left: Calibration line for 4-cyanophenol (4-CP) in solution; relative standard error of estimation (SEE) over the concentration range is 4.36%; relative standard error of performance (SEP) over the concentration range is 5.74%; $r^2 = 0.978$. Right: Calibration line for econazole nitrate (EN) in solution; SEE = 4.73%, SEP = 6.38%, $r^2 = 0.974$.

with 75% ACN for HPLC analysis, so the same solution composition was compared by NIR. Samples were placed inside the instrument drawer and scanned on top of a 135° conical reflecting cup to maximize light collection by the integrating sphere and detector. Each sample was scanned three times and rotated 120° between each subsequent scan. For data analysis, data were divided into their respective groups.

Saturated Solutions and Creams on Skin. Exposure times for EN solutions were 2 min, 2 h, and 15 h, EN creams were 2, 8.5, and 15 h, and exposure times for 4-CP were 2 min, 10 min, and 1 h. Following exposure to drug treatment, skin samples were removed from the MPD, the drug-exposed skin section (approximately 1.0 cm in diameter) was excised, and the surface formulation was carefully removed, loaded on a one-well depression slide, and covered with a cover slip (Gold Seal Products). NIR spectra were collected from covered skin samples. Samples were placed inside of the instrument drawer and on top of the conical reflecting cup and scanned three times each, rotating them 120° between each scan. For the data analysis, data were divided into their four respective groups: EN epidermis (outside/donor surface facing NIR probe), EN dermis (inside/receiver surface facing NIR probe), CP epidermis, and CP dermis.

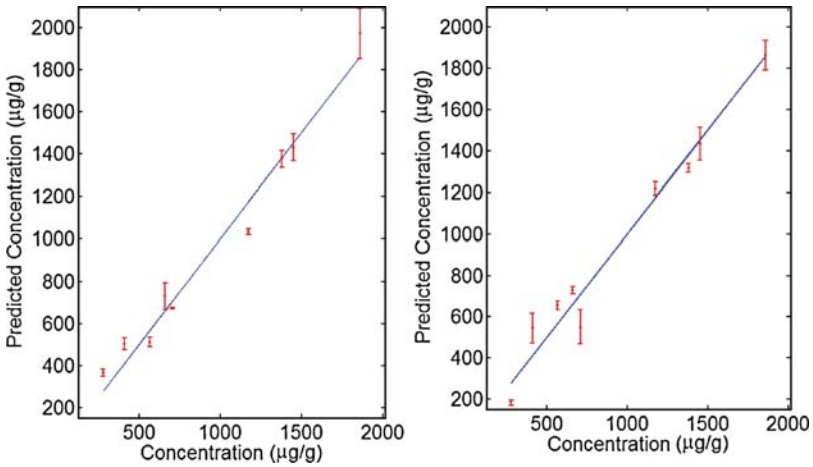

Fig. 2. Near-infrared (NIR) calibration line from skin samples treated with an applied dose of saturated EN in propylene glycol; left: epidermis calibration, SEE = 4.95%, SEP = 6.28%, $r^2 = 0.965$; right: dermis calibration, SEE = 4.77%, SEP = 6.73%, $r^2 = 0.959$. The calibration line is based on the leave-one-out cross-validation using the high-pressure liquid chromatography (HPLC) concentrations for the regression. The diagonal line is the mean of the HPLC results, and the error bars are the means and the standard errors of the NIR predictions.

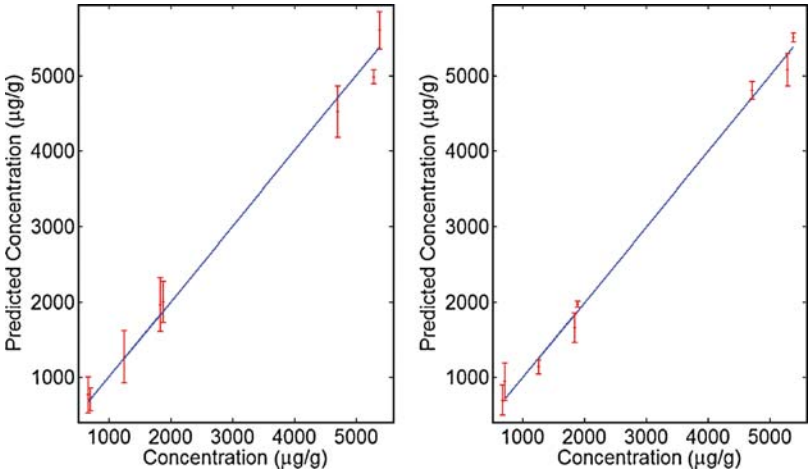

Fig. 3. NIR calibration line from skin samples treated with an applied dose of saturated 4-CP in water; left: epidermis calibration, SEE = 7.31%, SEP = 9.17%, r^2 = 0.917; right: dermis calibration, SEE = 5.51%, SEP = 6.84%, r^2 = 0.973. The diagonal line is the mean of the HPLC results, and the error bars are the means and the standard errors of the NIR predictions.

Data Analysis Method. To eliminate baseline variation because of different tissue thicknesses and sample preparation techniques, all data were multiplicative scatter-corrected (21). Data were presmoothed with a cubic spline operation. The following chemometric processing was applied to each of the data sets individually. From the scatter-corrected NIR spectra, principal components were calculated (16). A multiple least-squares regression identified the PCs that correlated most highly with the reported drug concentrations from the HPLC analysis. These components were used in a leave-one-out cross-validation to determine how effectively the NIR method predicted drug concentrations from the spectra. To find the most effective data analysis method, PCR was compared with iPCR and PCR-UVE.

Testing for Interferences. To prove that the strong correlations between HPLC and NIR were not artifacts and were in fact coming from 4-CP and EN, the contributions of solvents, drug vehicles, and placebo cream were evaluated and appropriate corrections were made. For example, normalized ACN and 25% buffer/PEG control spectra were subtracted from the 4-CP and EN solution spectra, and statistical analysis was repeated. The solvent-corrected spectra still demonstrated a high correlation to known concentrations, suggesting that the effects were entirely because of the analyte of interest. In addition, the absence of the

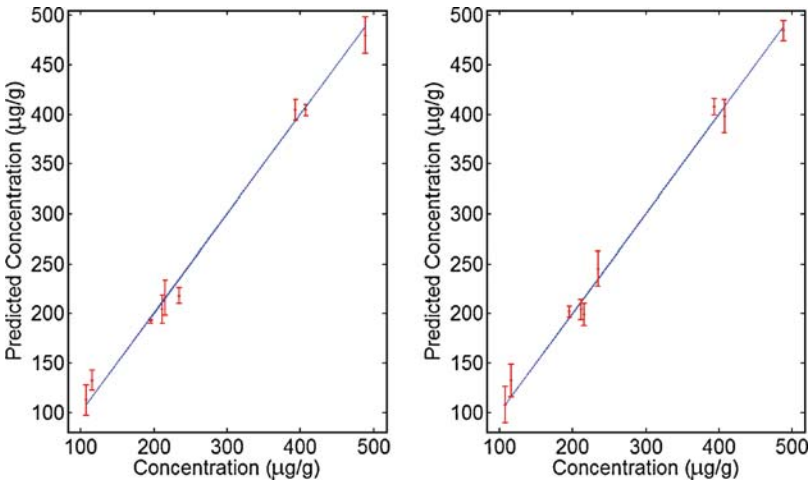

Fig. 4. NIR calibration line from skin samples treated with an applied dose of 0.4-ml Clay Park (1% EN); left: epidermis calibration, SEE = 4.16%, SEP = 5.39%, r^2 = 0.975; right: dermis calibration, SEE = 4.17%, SEP = 5.05%, r^2 = 0.978. The diagonal line is the mean of the HPLC results, and the error bars are the means and the standard errors of the NIR predictions.

Table I. HPLC and NIR Clay Park Cream Measurements

Exposure time (h)	Tissue number	HPLC (μg/g)	NIR (μg/g)	NIR Standard error	HPLC–NIR Correlation
2	1	216	249	17.3	0.867
		216	191		0.886
		216	207		0.956
2	2	196	194	1.64	0.992
		196	192		0.979
		196	189		0.963
2	3	394	413	7.18	0.955
		394	416		0.946
		394	383		0.972
8.5	4	116	149	10.5	0.780
		116	136		0.854
		116	113		0.973
8.5	5	235	223	10.5	0.948
		235	228		0.970
		235	202		0.862
8.5	6	489	494	18.1	0.991
		489	501		0.975
		489	444		0.907
15	7	408	394	5.81	0.966
		408	414		0.985
		408	404		0.989
15	8	212	227	14.2	0.936
		212	207		0.978
		212	178		0.838
15	9	108	143	15.6	0.755
		108	101		0.931
		108	93		0.863

This table presents the skin concentrations from a 0.4-ml applied dose of 1% Clay Park cream at three different exposure times as measured by the HPLC and NIR, and the strength of correlation between the two analytical instruments. Each tissue was scanned three times in the NIR prior to HPLC analysis.

solvent peaks allowed for the identification of the most significant regions in the NIR spectrum for the quantification of each drug. Rather than using a full-spectrum approach where the likelihood of chance correlations is higher, these specific wavelength regions were used for the quantification of each drug for saturated solution and cream experiments. In its identified wavelength region, the EN cream demonstrated a high correlation to HPLC concentrations, whereas at the same region, there was no predictive ability for the placebo cream, proving this was the correct region.

RESULTS

Interval PCR with 200 wavelengths resulted in the best standard errors of performance. Leardi and Norgaard (17) suggest that the inclusion of more variables increases the likelihood of overfitting and chance correlations. For 4-CP, the region spanning 1470–1870 nm demonstrated the highest correlation to HPLC concentrations, and for EN, the best region spanned 1936–2336 nm. Therefore, these regions were selected for all quantification experiments. Figures 1–4 illustrate calibration curves for 4-CP and EN in solution and in tissue. NIR spectroscopy successfully predicted the concentration of both types of analytes in solution, as shown in Fig. 1. The left side of Fig. 1 illustrates that NIR analysis of 4-CP in solution gives a relative standard error of estimation (SEE) over the concentration range of 4.36%, relative SEP over the concentration range of 5.74%, and $r^2 = 0.978$. The right side of Fig. 1 illustrates that NIR analysis of EN in ACN/PEG gives an SEE = 4.73%, SEP = 6.38%, and $r^2 = 0.974$.

Figure 2 (left) illustrates that the epidermal NIR calibration line from skin samples treated with an applied dose of saturated EN in propylene glycol gave an SEE = 4.95%, SEP = 6.28%, and $r^2 = 0.965$. Figure 2 (right) illustrates that the dermal NIR calibration line gave an SEE = 4.77%, SEP = 6.73%, and $r^2 = 0.959$. These calibration lines were based on the leave-one-out cross-validation using the HPLC concentrations for the regression.

Skin samples treated with an applied dose of saturated 4-CP in water and scanned from the epidermal side gave an SEE = 7.31%, SEP = 9.17%, and $r^2 = 0.917$, shown in Fig. 3 (left). The same samples scanned from the dermal side gave an SEE = 5.51%, SEP = 6.84%, and $r^2 = 0.973$, shown in Fig. 3 (right).

The most important results obtained are in Fig. 4 and Tables I and II, showing the excellent correlation of the 1% EN cream-treated skin data (analyzed by NIR) with the reference HPLC assay. Skin samples treated with an applied dose of 0.4 ml Clay Park (1% EN) scanned from the epidermis gave an SEE = 4.16%, SEP = 5.39%, and $r^2 = 0.975$, shown in Fig. 4 (left). The same samples scanned from the dermis gave an SEE = 4.17%, SEP = 5.05%, and $r^2 = 0.978$, shown in Fig. 4 (right). An expanded list of Clay Park results

Table II. The Strength of Correlation Between the HPLC and NIR for the Four Different Brands of Econazole Nitrate Creams Tested

	Spectazole®		Clay Park		Taro		Fougera	
Cream brand	Epidermis	Dermis	Epidermis	Dermis	Epidermis	Dermis	Epidermis	Dermis
r^2	0.957	0.931	0.975	0.978	0.936	0.961	0.934	0.960
SEE	5.46	6.53	4.16	4.17	7.42	5.38	7.36	5.78
SEP	6.43	8.17	5.39	5.05	8.94	6.95	8.97	6.96

The statistics [r^2, standard error of estimation (SEE), and standard error of performance (SEP)] come from a leave-one-out cross validation.

are given in Table I, and concise results for the other three creams are given in Table II. It is this proof of concept data that leads us to believe that it will be possible to analyze many other topical drug products using an NIR SSSI. Additionally, we are not limited by NIR because UV, VIS, and NIR LEDs plug into the SSSI and are easily changed.

DISCUSSION

Great Flexibility and Durability. This experiment applied NIR spectroscopic analysis in four distinct applications: drug powders, drug in solution, and tissue concentrations of drug after exposure to solutions and creams. The relative standard errors of performance and estimation and the strong correlation of NIR concentration prediction to the HPLC results suggest that NIR spectrometry is a flexible technique for analysis of tissue concentrations of drugs and other chemicals after topical exposure. In total, 270 NIR spectra were collected from skin samples. Only two spectra were discarded because of anomalous scans (short noise spikes from instrument preamplifier), suggesting that NIR is a very durable instrument.

NIR is also a nondestructive and rapid method of analysis, taking less than 2 min to complete a scan. No special sample preparation is required. In this research, samples were simply placed on a microscope slide and scanned. NIR also has the capability of being a noninvasive method of analysis. Using a fiber-optic probe, it is possible to scan skin tissue *in vivo* in whole animal or clinical studies. In this case, skin samples were scanned inside the instrument drawer; thus, external light and room noise were not a factor. In the drawer configuration, NIR spectra are essentially free from external noise and interference. Freedom from interference can be measured. An NIR "contaminant" spectrum (e.g., EN in the presence of trace amounts of 4-CP) can be mathematically translated in hyperspace toward one of the drugs until the two are chemically indistinguishable by the BEST metric (22). Spectra from similar samples tend to cluster in the same region of hyperspace; thus, pure component spectra cluster in distinct regions. The space between the two cluster centers is composed of theoretical mixtures of the two components. The distance that one cluster is translated toward the other before they are spatially indistinguishable corresponds to the theoretical NIR detection limit. When applied to EN and 4-CP, this operation indicated that both clusters were mathematically distinguishable until the mixture consisted of 98.0% contaminant.

The success of this phase of the experiments suggests the utility of a new portable NIR sensor for the rapid and accurate *in vivo* measurement of dermal absorption and topical bioequivalence (23). The concentric circle design of a new NIR SSSI allows the instrument to focus on all tissue depths simultaneously. When a scan is collected from the epidermal side, the signal detected from the innermost circle reflects tissue scattering events only from the surface. However, the signal detected from the middle circle reflects tissue scattering events from both the surface and a moderate number of skin layers. Likewise, the signal detected from the outermost circle reflects tissue scattering events from all depths simultaneously. With this information in hand, the inner and middle circles can be used as reference channels, and their drug spectra can be subtracted to yield pure interference-free spectra at lower depths. Removal of formulation prior to scanning tends to be highly variable; however, the SSSI will make it possible to measure drug penetration at lower tissue depths without removing formulation from the surface.

CONCLUSION

As the use of topical dosage forms becomes more common, the need has arisen for an analytical method capable of noninvasively assessing dermal absorption and topical bioequivalence. This research demonstrates that for the rapid and accurate measurement of topical bioequivalence of EN formulations, NIR spectrometry is an analytical method worth further exploration. A portable NIR instrument is currently under construction that provides for depth profiling at a number of discrete NIR wavelengths based on a CW experiment format using spatial feature encoding and integrated computational imaging (24). With an array of LEDs, and the use of frequency modulation, all wavelengths are collected simultaneously. The instrument is designed so that an NIR spectrum is collected at various depths in the skin sample and so that the experimenter can locate a spectral signature at different depths in the sample. With this design, the entire analysis takes merely 15 seconds, eliminating the problem of thermal drift and chemical evaporation.

ACKNOWLEDGMENT

This research was sponsored by the Food and Drug Administration, contract number D3922004.

REFERENCES

1. V. P. Shah, D. Hare, S. V. Dighe, and R.L. Williams. Bioequivalence of topical dermatological products. *Top. Drug Bioavailab., Bioequiv., Penetration*, 1993, 393–413.
2. J. Traulsen. Bioavailability of betamethasone dipropionate when combined with calcipotriol. *Int. J. Dermatol.* **43**(8):611–617 (2004).
3. L. K. Pershing, J. L. Nelson, J. L. Corlett, S. P. Shrivastava, D. B. Hare, and V. Shah. Assessment of dermatopharmacokinetic approach in the bioequivalence determination of topical tretinoin gel products. *J. Am. Acad. Dermatol.* **48**(5):740–751 (2003).

4. F. Pirot, Y. N. Kalia, A. L. Stinchcomb, G. Keating, A. Bunge, and R. H. Guy. Characterization of the permeability barrier of human skin *in vivo*. *Proc. Natl. Acad. Sci. USA* **94**:1562–1567 (1997).
5. A. L. Stinchcomb, F. Pirot, G. D. Touraille, A. L. Bunge, and R. H. Guy. Chemical uptake into human stratum corneum *in vivo* from volatile and non-volatile solvents. *Pharm. Res.* **16**(8):1288–1293 (1999).
6. M. B. Reddy, A. L. Stinchcomb, R. H. Guy, and A. L. Bunge. Determining dermal absorption parameters *in vivo* from tape strip data. *Pharm. Res.* **19**(3):292–298 (2002).
7. M. Kreilgaard, M. B. Kemme, J. Burggraaf, R. C. Schoemaker, and A. F. Cohen. Influence of a microemulsion vehicle on cutaneous bioequivalence of a lipophilic model drug assessed by microdialysis and pharmacodynamics. *Pharm. Res.* **18**(5): 593–599 (2001).
8. C. Xiao, D. J. Moore, M. E. Rerek, C. R. Flach, and R. Mendelsohn. Feasibility of tracking phospholipid permeation into skin using infrared and Raman microscopic imaging. *J. Invest. Dermatol.* **124**(3):622–632 (2005).
9. M. Cope and D. T. Delpy. System for long-term measurement of cerebral blood and tissue oxygenation on newborn infants by near-infrared transillumination. *Med. Biol. Eng. Comput.* **26**:289–294 (1988).
10. B. Chance, J. S. Leigh, H. Miyake, D. S. Smith, S. Nioka, R. Greenfeld, M. Finander, K. Kaufmann, W. Levy, M. Young, P. Cohen, H. Yoshioka, and R. Boretsky. Comparison of time-resolved and -unresolved measurements of deoxyhemoglobin in brain. *Proc. Natl. Acad. Sci. USA* **85**:4971–4975 (1988).
11. A. H. Gandjbakhche and G. H. Weiss. *Prog. Opt.* **XXXIV**: 335–402 (1995).
12. G. H. Weiss. Some applications of persistent random walks and the telegrapher's equation. *Physica, A* **311**:381–410 (2002).
13. A. Urbas, M. W. Manning, A. Daugherty, L. A. Cassis, and R. A. Lodder. Near-infrared spectrometry of abdominal aortic aneurysm in the ApoE−/− mouse. *Anal. Chem.* **75**:3650–3655 (2003).
14. R. J. Dempsey, D. G. Davis, R. G. Buice, and R. A. Lodder. Biological and medical applications of near-infrared spectroscopy. *Appl. Spectrosc.* **50**:18A–34A (1996).
15. L. A. Cassis and R. A. Lodder. Near-IR imaging of atheromas in living arterial tissue. *Anal. Chem.* **65**:1247–1256 (1993).
16. I. T. Jolliffe. *Principal Component Analysis*, Springer, New York, 2002.
17. R. Leardi and L. Norgaard. Sequential application of backward interval partial least squares and genetic algorithms for the selection of relevant spectra regions. *J. Chemom.* **18**:486–497 (2004).
18. O. E. Noord. Elimination of uninformative variables for multivariate calibration. *Anal. Chem.* **68**:3851–3858 (1996).
19. L. Ferry, G. Argentieri, and D. Lochner. The comparative histology of porcine and guinea pig skin with respect to iontophoretic drug delivery. *Pharm. Acta Helv.* **70**:43–56 (1995).
20. R. A. Lodder, M. Selby, and G. Hieftje. Detection of capsule tampering by near-infrared reflectance analysis. *Anal. Chem.* **59**:1921–1930 (1987).
21. P. Geladi, D. MacDougall, and H. Martens. Linearization and scatter-correction for near-infrared reflectance spectra of meat. *Appl. Spectrosc.* **39**(3):491–500 (1985).
22. R. A. Lodder and G. Hieftje. Detection of subpopulations in near-infrared reflectance analysis. *Appl. Spectrosc.* **42**(8):1500–1512 (1988).
23. J. Medendorp, J. Yedluri, A. Stinchcomb, and R. Lodder. A portable near-infrared sensor for noninvasively measuring drug concentrations in the skin after topical application. *AAPS J.* **7**(S2) 2005.
24. L. A. Cassis, A. Urbas, and R. A. Lodder. Hyperspectral integrated computational imaging. *Anal. Bioanal. Chem.* **382**:868–872 (2005).